

University of Groningen

Intramolecular triplet-state quenching as a general method for photostabilization

van der Velde, Jasper Hendrik Martinus

IMPORTANT NOTE: You are advised to consult the publisher's version (publisher's PDF) if you wish to cite from it. Please check the document version below.

Document Version

Publisher's PDF, also known as Version of record

Publication date:

2016

[Link to publication in University of Groningen/UMCG research database](#)

Citation for published version (APA):

van der Velde, J. H. M. (2016). Intramolecular triplet-state quenching as a general method for photostabilization. [Groningen]: Rijksuniversiteit Groningen.

Copyright

Other than for strictly personal use, it is not permitted to download or to forward/distribute the text or part of it without the consent of the author(s) and/or copyright holder(s), unless the work is under an open content license (like Creative Commons).

Take-down policy

If you believe that this document breaches copyright please contact us providing details, and we will remove access to the work immediately and investigate your claim.

Downloaded from the University of Groningen/UMCG research database (Pure): <http://www.rug.nl/research/portal>. For technical reasons the number of authors shown on this cover page is limited to 10 maximum.

Introduction

Fluorescence microscopy has become a widely used tool within all natural sciences and is a powerful technique for the study of cells, tissues but also polymers, organic and inorganic materials. Here, engineered luminescent materials are used as molecular probes reporting on the structure, dynamics and chemical properties of the sample.

During the last decades the optical detection of single molecules¹ has become possible and is nowadays used to determine the position, translational motion and conformational dynamics of single biomolecules, examples include movement of single motor proteins^{2,3}, diffusion of lipid molecules in membranes^{4,5}, RNA folding and catalysis⁶⁻⁸ and the transport of molecules or ions across the membrane both *in vivo*⁹ and *in vitro*¹⁰. Where ensemble techniques yield an average value of an observable, the study of single molecules reveals the complex behavior and heterogeneity of biomolecules. These techniques provide an unprecedented insights into the working mechanism of macromolecules¹¹⁻¹³, even with a resolution that exceeds that of conventional light microscopy (super-resolution microscopy)^{1,14-17}. In 2014 the "Nobel Prize for Chemistry" was awarded for the development of super-resolved fluorescence microscopy, allowing to overcome the physical diffraction limit of light (< 250 nm), *via* use of luminescent materials.

The rapid developments in the use of fluorescent techniques were accompanied by similar progress in the design of the fluorescent probes, *i.e.*, distinct photophysical and chemical properties of the probes. Especially, with the progress of detectors and optics reaching high detection efficiencies, future advancements in fluorescence microscopy currently depend on further improvements of the fluorescent probes.

Fluorescent labels

In fluorescence microscopy, the emission of luminescent labels is detected down to the sensitivity of single molecules via the absorption and subsequent emission of a photon. Although natural macromolecules contain fluorescent sources such as aromatic amino acids (for example tryptophan, tyrosine and phenylalanine), most proteins and nucleic acids do not show considerable fluorescence due to their low absorption cross-section, quantum yield ($< 0.01 - 0.35$) and photostability. Their weak UV emission is not useful for sensitive fluorescence detection down to the single molecule level. Only natural chromophores such as green fluorescent protein^{18,19} are actually suitable for single molecule detection.

The most commonly used labels in biophysics that are attached to the molecules of interest are fluorescent proteins^{18,19}, quantum dots^{20,21} and organic fluorophores^{12,14,15,22,23}. These "extrinsic" fluorescent labels have the advantage that they can be tuned in absorption and emission properties across the visible spectrum, ranging from the near-ultraviolet into the near-infrared. Ideally, these fluorescent probes have high molar absorption coefficients ($> 10^4$ M⁻¹·cm⁻¹), quantum yields (> 0.1), and show a bright and fluorescent signal over longer time periods. In the end the interpretation and quality of fluorescent signals is directly linked to the number of available

photons, limiting signal to noise ratio and observation time.

Fluorescent proteins have revolutionized biological (live) cell imaging. They are small with a typical size of $\sim 2.5\text{-}4$ nm (25-30 kDa). They can be genetically encoded fluorescent and used for single molecule and super-resolution microscopy applications. Green fluorescent protein (GFP) is most known¹⁸ with a structure characterized as a rigid 11-sheet beta-barrel with a center helix. Inside this center helix the chromophore 4-(p-hydroxybenzylidene)-5-imidazolinone is formed from a tripeptide¹⁸. Despite, ongoing efforts to improve the physical and chemical properties of fluorescent proteins they rather show poor photophysical properties, intrinsic signal fluctuations in the fluorescent emission (blinking) resulting in low brightness and fast photodegradation²⁴⁻³⁰.

On the contrary, quantum dots (semiconducting materials) exhibit a high quantum yield, narrow emission spectrum complemented with a broad excitation spectrum and high photostability making them particularly useful for long-lasting fluorescence experiments^{20,21}. Quantum dots are, however, rather large ($\sim 10\text{-}100$ nm) especially when made water-soluble. Consequently, interference with biological function and toxicity to cells limits their use; nevertheless they are particularly useful for single molecule particle tracking. On/off transitions in the fluorescent emission of quantum dots are characterized^{31,32} and efforts have been made to synthesize a non-blinking quantum dot³².

Synthetic organic fluorophores are among all available fluorescent labels a popular choice and they have become a major driving force for the recent success of fluorescence-based methods^{12,22,33}. Synthetic organic fluorophores are characterized by conjugated alternating single and double bonds (Figure 1.1). Most importantly, the size of organic fluorophores is considerably smaller ($\sim 1\text{-}2$ nm) than fluorescent proteins and quantum dots, thereby showing minimum influence on the system of interest. A variety of different organic fluorophores exist (Figure 1.1), with specific physical and chemical properties. Labeling of biochemical targets is realized by linking chemistry using different reactive functional groups. Additionally, great efforts have been made

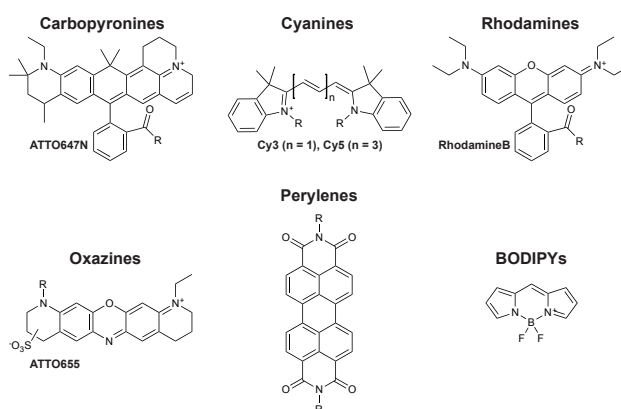


Figure 1.1 | Typical classes of organic fluorophores used in single-molecule studies: carborhodamines (ATTO647N), cyanines (Cy3 and Cy5), rhodamines (RhodamineB), oxazines (ATTO655), perylenes and BODIPYs (general core structures shown).

to allow use of organic fluorophores inside (living) cells^{34–36}.

Especially single molecule fluorescence and super-resolution techniques pose stringent demands on the organic fluorophores which are pushed to the limit of their physical and chemical properties, that is, being water soluble, chemically inert and stable emission. However, as for all labels discussed here, synthetic organic fluorophores intrinsically suffer from transient excursions to dark states ("blinking") causing signal fluctuations. Fast irreversible destruction ("photobleaching") results in a limited observation window of the system of interest and is another major problem for synthetic organic fluorophores^{22,23}. Both blinking and photobleaching have various origins but are influenced heavily by the presence of oxygen and photoinduced electron transfer reactions^{22,37–40}.

Intrinsic signal fluctuations and photobleaching of organic fluorophores

Photophysical and -chemical processes of synthetic organic fluorophores start in the electronic ground state of a fluorophore, referred to as S_0 (Figure 1.2). S_0 has an anti-parallel spin configuration giving rise to the singlet nature. Light of appropriate wavelength ($\lambda_{ex} = h\nu$) stimulates transitions to higher electronic states (S_n). For light with appropriate energy, a transition from the singlet ground state (S_0) to the first excited singlet state (S_1) takes place (Figure 1.2, rate k_{ex}), via fast photon absorption and excitation is ($\sim 10^{-15}$ s). Due to this fast electronic transition, which is faster than nuclear motion, the "frozen" nuclei (Frank-Condon principle) equilibrates via vibrational relaxation (rate k_{vib}) into the vibrational ground state of S_1 on the picosecond timescale $\sim 10^{-12}$ s

A fluorophore residing in the first excited state can return to the singlet ground state via different processes. Either via a non-radiative process called internal conversion (rate k_{IC} , Figure 1.2), transferring the excess energy to populate vibrational states of the S_0 state as heat to the solvent molecules. Alternatively, conversion from the first excited singlet state S_1 to the singlet ground state with the joint emission of a photon (fluorescence) can occur (rate k_f , Figure 1.2). Typically, fluorescence results in the emission of a photon of lower energy ($\lambda_{fl} = h\nu < \lambda_{ex}$, Stokes shift)). Fluorescent lifetimes are on timescales on the order of nanoseconds (10^{-10} - 10^{-9} s)^{23,41}. The efficiency of absorption and emission of photons depends on the intensity of the excitation (I_{ex}) light and the absorption coefficient of the organic fluorophore. The ratio between the number of emitted and absorbed photons is called fluorescence quantum yield.

If this process is repeated a single molecule will emit continuously. However, besides a (non-)radiative conversion from the single excited state to the singlet ground state, a spin forbidden transition to the triplet manifold can occur. The triplet state (T_1) is populated via a process called inter-system crossing (rate k_{ISC} , Figure 1.2). The inter-system crossing rate, k_{ISC} , for organic fluorophores is typically low (quantum yield < 0.01). Triplet states typically show a lifetime on the order of micro- to milliseconds (10^{-6} - 10^{-3} s). The decay of the triplet state can

occur via different processes; a non-radiative process or conversion with the concomitant emission of a photon called phosphorescence. Since, phosphorescence is a spin forbidden transition it occurs on time scales much longer than fluorescence and does not contribute to the overall emission signal. Transitions into the triplet state are therefore seen as on/off transitions in the emission of a single molecule (triplet-blinking).

Effectively, the triplet state can be considered as a non-fluorescent state with a long lifetime. Due to the chemical nature with two unpaired electrons and the excess energy makes that the triplet state is chemically reactive, such as electron transfer reactions (redox reactions) yielding radicals ($F^{\cdot-}$ and $F^{\cdot+}$, both dark states, Figure 1.2). From the radical states the molecule can either return to the singlet ground state via complementary redox reactions or towards a photobleached product (**P**, rate k_P , Figure 1.2). This significantly reduces the observation times of the fluorescence of organic fluorophores (photobleaching).

Photobleaching can occur via various chemical pathways and remains a complicated phenomenon to be understood. The following section explains different possible photobleaching pathways catalyzed by oxygen. Molecular oxygen has a triplet ground state (3O_2) and is present at millimolar concentrations (~ 0.3 mM)^{14,42-44} in aqueous buffer systems and it is one of the major causes for photobleaching of organic fluorophores (Figure 1.2). Energy transfer from the triplet state towards oxygen via triplet-triplet annihilation leads to the formation of excited singlet oxygen (1O_2) and the fluorophore in the ground state (rate k_{O_2} , Figure 1.2). Additionally, molecular oxygen can directly react with the triplet state of the fluorophore causing an electron

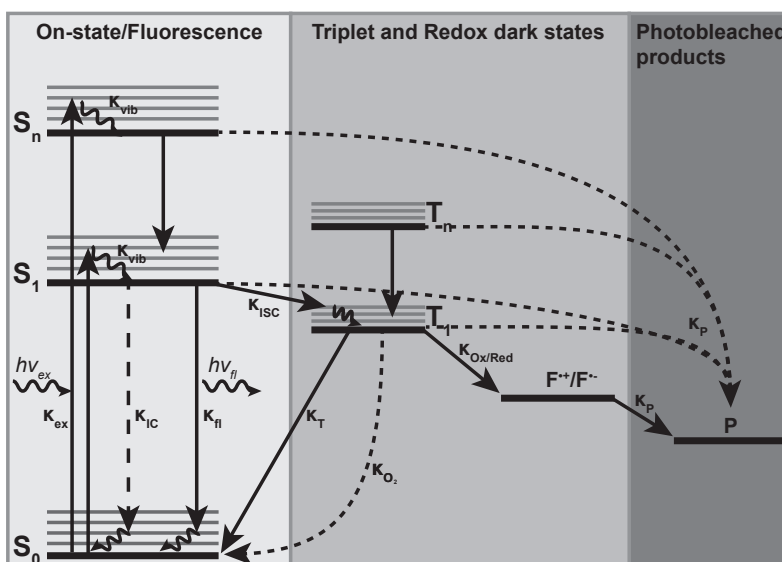


Figure 1.2 | Jablonski diagram of the underlying photophysical description of a synthetic organic fluorophore. S_0 is the ground state of the fluorophore; S_1 is the first excited singlet state; S_n are higher order excited singlet states; T_1 is the first excited triplet state; T_n are higher order excited triplet states; $F^{\cdot+}$ is the cationic radical state; $F^{\cdot-}$ is the anionic radical state; **P** is the photobleached state.

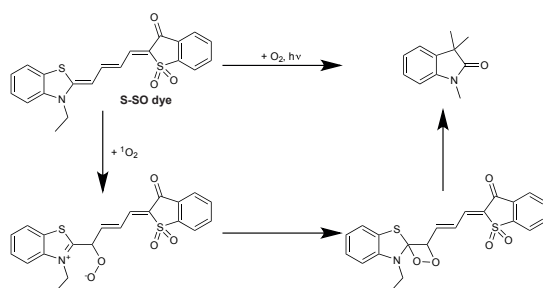


Figure 1.3 | Photooxidation of **S-SO** dye via and initial ¹O₂ attack. (Figure adapted from Touthkine *et al.*⁴⁵)

transfer reaction with the joint formation of a radical cation of the fluorophore and a radical superoxide. Both oxygen species can react with the fluorophore leading to photobleaching and short fluorescent observation times (Figure 1.4a). The mechanism of photooxidation **S-SO** dyes is well characterized (Figure 1.3)⁴⁵. First triplet-triplet energy of the **S-SO** dye and ³O₂ yields the production of reactive electrophilic ¹O₂. Initial attack of ¹O₂ on the polymethine chain yields a dioxetane. Subsequent cleavage of the dioxetane results in the formation of carbonyl groups. Similar reaction pathways are believed to occur for other classes of organic fluorophores. Besides photobleaching of the fluorophore, reactive oxygen species can react with (bio-)molecular targets resulting destruction of the system of interest^{46–48}.

Removal of oxygen

In aqueous buffer systems the triplet state lifetime can reach milliseconds causing distinct on/off transitions in the fluorescence of a single molecule (Figure 1.4). However, the presence of oxygen in saturated air solutions results in efficient triplet quenching reducing the lifetime down to microseconds (rate k_{O_2} , Figure 1.2b). Typically, the triplet quenching rate of oxygen is close to the diffusion limit, $>10^6 \text{ s}^{-1}$ ⁴⁹, which is significantly faster than the rate of formation of the fluorophore radical states.

Despite being an efficient triplet-state quencher, oxygen and related reactive oxygen species react with the fluorophore leading to photobleached products. To prolong the lifetime of organic fluorophores it is essential to remove oxygen. Enzymatic oxygen-scavenging systems like a glucose-oxidase/catalase (GOC) combination or protocatechuic acid and protocatechuate-3,4-dioxygenase (PCA/PCD) are most commonly used to remove oxygen^{43,50,51}. In enzymatic oxygen-scavenging systems oxygen is consumed for the oxidation of the substrate (glucose or 3,4-protocatechuic acid, respectively). In a closed system the concentration of oxygen in aqueous solutions can be reduced to micromolar concentrations⁴³, without possible replacement of O₂ from the surroundings.

The removal of oxygen can lead to prolonged photobleaching times of the organic fluorophores by removing the reactive oxygen species but at the same time it also results in an increased lifetime of the triplet-state. As a result, the fluorescence of a single molecule shows pronounced

on/off transitions with the off-times corresponding to the triplet-state lifetime (Figure 1.4). To account for the removal of oxygen with the joint increase in triplet-state lifetime, triplet state quenchers are added^{22,37-40,52-54}.

Triplet-state quenchers as solution additives and a reducing oxidizing system (ROXS)

To efficiently remove the blinking of triplet-related dark states and prolong the fluorescence photobleaching time, solution additives can be added that quench the triplet state^{22,37-40,52-54}. Different quenching mechanisms are used to obtain ideal fluorescent time traces as depicted in Figure 1.4c. The general idea is to replace molecular oxygen as the triplet state quencher with a compound that do not generate chemically reactive species as a result of triplet quenching.

In the line of quenching the triplet and protecting the fluorophore from reactive oxygen species β -mercaptoethanol⁵⁵ (an antioxidant) was first used. Not long after other compounds were empirically found to more efficiently quench the triplet state in the absence of oxygen or protect the fluorophore from the generation of reactive oxygen species in the presence of oxygen, for example β -mercaptoethylamine⁵⁶, L-glutathione^{52,54}, n-propyl galate⁵⁷, ascorbic acid^{52,58}, and 1,4-diazabicyclo[2,2,2]octane (DABCO)⁵⁹.

Photoinduced electron transfer (PET) allows rational design of quenching *via* formation of radical states (\mathbf{F}^- and \mathbf{F}^+) originating mostly from the triplet state (rate k_{Red} and k_{Ox} Figure 1.2 and Figure 1.4d)^{22,37-40,52-54,60}. Via this method the triplet state lifetime gets efficiently reduced. However, as mentioned both triplet and radical states are prone to reactions leading to photobleaching (rate $k_{P\cdot}$, k_{P^*} and $k_{P^{**}}$). To reduce the lifetime of the radical states, a follow up redox reaction needs to take place converting the fluorophore back to the singlet ground state^{39,40}. Upon removing oxygen and adding a reducer and oxidizer a so-called reducing and oxidizing system (ROXS) is created³⁹. Using ROXS, the triplet state of the fluorophore gets quenched via a reduction (rate k_{Red}) or oxidation (rate k_{Ox}), reaction yielding a radical cat- or anion (\mathbf{F}^- and \mathbf{F}^+ , Figure 1.4d). Subsequent oxidation (rate $k_{Ox'}$), or reduction (rate $k_{Red'}$), reaction, depending on the formed radical, brings the fluorophore back to the singlet ground state. Using ROXS the lifetimes of the triplet and radical states are significantly reduced and the photobleaching is less efficient ($k_{P\cdot}$, k_{P^*} and $k_{P^{**}}$) due the to the rate of oxidation and reduction that is larger than the rate of the pathways leading to the photobleached products.

The combination of ascorbic acid (AA) and methyl viologen (MV) has proven to work systematically in quenching the triplet state, and thereby efficiently competing with the rate of photobleaching³⁹, for a variety of organic fluorophores. The addition of both the oxidizer (AA, vs. SCE $E_{Ox} = 0.06 \text{ V}^{61}$) and reducer (MV, vs. SCE $E_{Ox} = -0.45 \text{ V}^{62}$) will not result in a ground state electron transfer reaction, as can be deduced from their redox potentials. However, after photon absorption by the fluorophore leading to a transition into the S_1 , sufficient energy is supplied to the system to allow for a redox cycle through the T_1 and radical ion states (\mathbf{F}^-

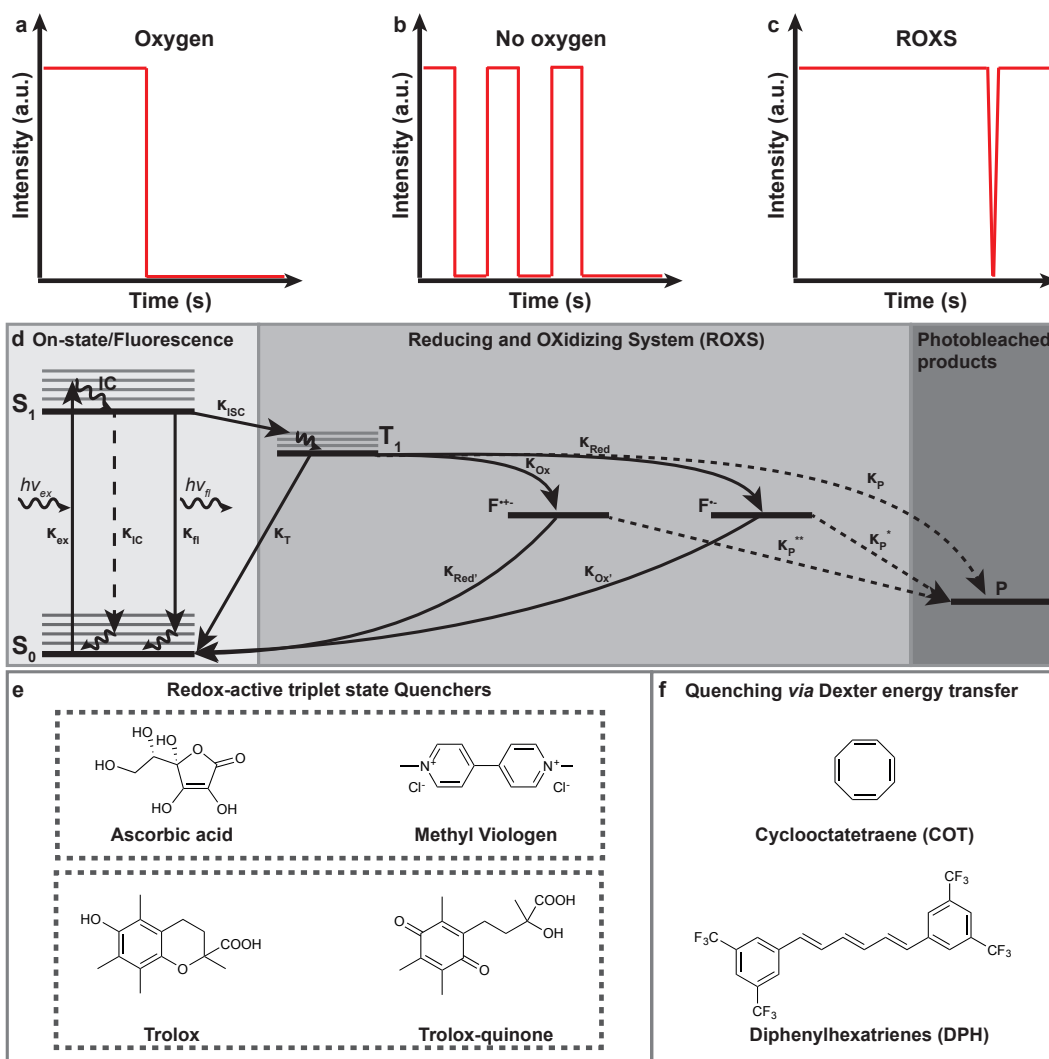


Figure 1.4 | Schematic representation of the fluorescence with triplet- and redox-blinking under (a) oxygen saturated buffer conditions, (b) de-oxygenated buffer conditions and (c) using a reducing and oxidizing system (ROXS). (d) Jablonski diagram of organic fluorophores including radical states. Upon excitation to the singlet excited state (S_1), non-radiative (k_{IC}) or radiative decay (k_{fl}) back the singlet ground state occurs (S_0). Occasionally ISC (k_{TSQ}) to the triplet state (T_1) occurs. When oxidizing and reducing compounds are added, either an oxidation (k_{Ox}) or reducing (k_{Red}) of the triplet state occurs yielding either radical cation ($F^{+\cdot}$) or radical anion ($F^{-\cdot}$), respectively. A follow up reduction or oxidation of the radical states yields the molecule back in the singlet ground state. Using ROXS the photobleaching pathways ($k_{P\cdot}$, $k_{P^{+\cdot}}$ and $k_{P^{-\cdot}}$) are suppressed^{39,40}. (e) Examples of redox active compounds (Ascorbic acid, Methyl Viologen, Trolox and Trolox-quinone) that can be added to reduce or oxidize the triplet state^{39,40,52}. (e) Examples of redox active compounds (Ascorbic acid, Methyl Viologen, Trolox and Trolox-quinone) that can be added to reduce or oxidize the triplet state^{39,40,52}. Combinations of a reducer and oxidizer (indicated in the dashed boxes) complete the ROX system. (**Continues next page**)

Figure 1.4 | (Continued) (f) Examples of compounds that quench the triplet state via Dexter type energy transfer mechanism (COT and Diphenylhexatrienes)⁵³. (Figure adapted from Ha *et al.*²²)

and \mathbf{F}^+) back to the S_0 .

Using the Rehm-Weller equation⁶³ (Equation 1.1) an approximation is made for the free energy change when using ROXS. In Equation 1.1 E_{ox} and E_{red} are the first 1-electron oxidation and reduction potentials of the donor and acceptor, respectively, $E_{0,0}$ is the zero-zero energy, e is the electron charge and C is the Coulombic attraction energy which is neglected here due to the high polarity of water.

$$\Delta G_{\text{CS}} = e[E_{\text{ox}} - E_{\text{red}}] - E_{0,0} + C \quad (1.1)$$

In Table 1.1 the the redox potentials for the dyes Cy5⁶⁴ and ATTO647N⁶⁵ (Figure 1.1) together with the free energy changes in each reaction step with either the reducer (MV) or oxidizer (AA) are shown. From the free energy changes it is clear that for both Cy5 as ATTO647N the reduction and oxidation reaction-steps from the T_1 are exothermic (negative free energy change). This supports the theory of the ROX system that the T_1 is quenched by a reducer and oxidizer, here AA and MV respectively. To recover the singlet ground state (S_0) a follow-up redox reaction with either of the radical ion states (\mathbf{F}^- and \mathbf{F}^+) needs to take place. Comparison of the reduction and oxidation potentials of the fluorophores with those of MV and AA, respectively, will give an indication of the free energy change for this charge recombination (Table 1.1, $\Delta G_{\text{red}'}$ and $\Delta G_{\text{ox}'}$). As shown in Table 1.1 all the reaction steps show exothermic free energy changes, thereby supporting the ROX system for quenching of the triplet-state and photostabilization via charge separated states (\mathbf{F}^- and \mathbf{F}^+).

Another well-known compound that works according to the ROXS mechanism is the vitamin E-derivative Trolox (TX). Trolox, an antioxidant (reducer), degrades upon dissolving in aqueous buffer solutions and form an oxidizing derivative called Trolox-quinone (TQ, oxidizer)⁴⁰. In Table 1.2 the redox potentials and free energy changes for each redox reaction with Trolox (TX, vs.

Dye	$E_{0,0}^S$ (V)	$E_{0,0}^T$ (V)	E_{red} (V)	E_{ox} (V)	$\Delta G_{\text{red}, S}$ (eV)
Cy5	1.88	1.60	-0.84	0.97	-0.98
ATTO647N	1.90	1.65	-0.64	1.11	-1.2
ATTO655	1.86	1.56	-0.42	1.31	-1.38

Dye	$\Delta G_{\text{red}, T}$ (eV)	$\Delta G_{\text{ox}, S}$ (eV)	$\Delta G_{\text{ox}, T}$ (eV)	$\Delta G_{\text{red}'}$ (eV)	$\Delta G_{\text{ox}'}$ (eV)
Cy5	-0.7	-0.46	-0.18	-0.91	-0.39
ATTO647N	-0.95	-0.34	-0.09	-1.05	-0.19
ATTO655	-1.08	-0.10	0.20	-1.25	0.03

Table 1.1 | Reduction and oxidation potentials for Cy5 and ATTO647N and corresponding free energy changes upon redox reactions from the T_1 with ascorbic acid (AA, vs. SCE $E_{\text{ox}} = 0.06$ V) and methyl viologen (MV, vs. SCE $E_{\text{red}} = -0.45$ V). All redox potentials were obtained by cyclic voltammetry^{39,61,62,64,65}.

Dye	$E_{0,0}^S$ (V)	$E_{0,0}^T$ (V)	E_{red} (V)	E_{ox} (V)	$\Delta G_{\text{red, S}}$ (eV)
Cy5	1.88	1.60	-0.84	0.97	-0.85
ATTO647N	1.90	1.65	-0.64	1.11	-1.07

Dye	$\Delta G_{\text{red, T}}$ (eV)	$\Delta G_{\text{ox, S}}$ (eV)	$\Delta G_{\text{ox, T}}$ (eV)	$\Delta G_{\text{red}^{\cdot}}$ (eV)	$\Delta G_{\text{ox}^{\cdot}}$ (eV)
Cy5	-0.57	-0.41 to -0.83	-0.13 to -0.55	-0.78	-0.34 to -0.76
ATTO647N	-0.82	-0.29 to -0.71	-0.04 to -0.46	-0.92	-0.14 to -0.56

Table 1.2 | Reduction and oxidation potentials for Cy5 and ATTO647N and corresponding free energy changes upon redox reactions from the T_1 with Trolox (TX, vs. SCE $E_{\text{ox}} = 0.19$ V) and Trolox Quinone (TQ, vs. SCE $E_{\text{red}} = -0.08$ to -0.50 V (estimated from structural similar quinones). All redox potentials were obtained by cyclic voltammetry^{39,40,64–66}.

SCE $E_{\text{ox}} = 0.19$ V⁴⁰) and Trolox-quinone (TQ, vs. SCE $E_{\text{ox}} = -0.08$ to -0.50 V (deduced from structural similar quinone structures)^{40,66}) are shown. From the values for the free energy changes it can be concluded that for Cy5 and ATTO647N Trolox and its quinone derivative can be used to efficiently quench the triplet and bring the fluorophore back to the singlet ground state (S_0) via the radical ion states ($\text{F}^{\cdot-}$ and $\text{F}^{\cdot+}$).

On the contrary, similar calculation for ATTO655, an oxazine dye with a high-lying reduction potential (Table 1.1) results in a positive free energy changes for oxidation and therefore a low rate for populating the radical cation states of ATTO655. Additionally, the reduced states of ATTO655 will not be efficiently depopulated by MV because of a calculated free energy change of $\Delta G_{\text{ox}^{\cdot}} = 0.03$.

As a result, for special cases, *i.e.*, with organic fluorophores known to have a low reduction potential (oxazines (see Table 1.1 for ATTO655) and perylenes) different concentrations of reducer and oxidizer can be used to independently tune the on and off times of one single emitter⁶⁸. Changing the concentration of reducer at constant oxidant concentration the on time of fluorescence can be adjusted independently since their reactivity is towards different states of the fluorophore. Changing the concentration of oxidant at constant reducer concentration the off time of the fluorescence can be adjusted. Consequently, at particular concentrations of oxidant and reducer the fluorescent emission shows predefined on and off times making it useful for stochastic readout super-resolution techniques, that is, the fluorescence of multiple emitters is temporally separated.

Besides redox-active triplet state quenchers, other chemical compounds can be added to deplete the triplet state via a triplet-triplet annihilation or Dexter energy transfer type mechanism (Cyclooctatetraene (COT) and Diphenylhexatriene (DPH) (Figure 1.4f))³⁷. Here, the electron in the triplet state is transferred to the lowest unoccupied state (LUMO) of COT or DPH. Back electron transfer from the highest occupied state (HOMO) of COT or DPH results in a fluorophore in the singlet ground state.

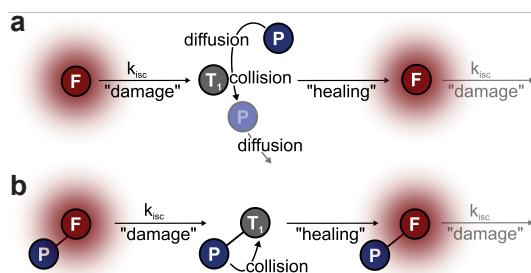


Figure 1.5 | Working principles of different methods for photostabilization of organic fluorophores. (a) Solution-based healing using collisional quenching with photostabilizers provided at high concentrations in the imaging buffer. (b) Self-healing using a single covalently attached photostabilizer, creating a high local concentration resulting in collisions between the fluorophore-triplet and the photostabilizer

Intramolecular photostabilization: "self-healing"

ROXS and other triplet state quenchers are effective buffer additives to stabilize different organic fluorophores (Figure 1.1 and Figure 1.4e,f). The efficiency of triplet quenching depends on the relative energy differences of the involved states of triplet state quenchers and fluorophore. In most single molecule experiments the solution additives are added at millimolar concentrations to enable sufficient number of collisions between photostabilizer and fluorophore. These conditions are incompatible with live-cell imaging and various *in vitro* systems. Also systems where collisions between fluorophore and photostabilizer are prohibited (Figure 1.5a) is problematic. In Green fluorescent protein (GFP) for example, where the chromophore is embedded within the protein, the collision-based model of diffusion-based triplet state quenching may be less efficient. Additionally, toxicity effect may play a role when redox active compounds react with the (bio)molecular targets or other components of the system of interest.

Lüttke and co-workers introduced covalent binding of triplet-state quenchers and singlet-oxygen scavengers to laser dyes in the 1980s as a strategy to prevent T-T absorption and photodamage caused by singlet oxygen (Figure 1.5b)^{69–71}. Despite having only a single protecting molecule attached to the laser-dye, the protecting mechanism can be repeated due to internal relaxation back of the protecting agent back to the ground state. Such an approach circumvents the previously mentioned disadvantages of diffusion based photostabilization.

In Figure 1.6 the laser dye POPOP and its photostabilizer-dye conjugates are shown. A triplet state quenching molecule was linked to POPOP laser dyes to depopulate the triplet state, here a *trans*-stilbenzine (**2** and **3** in Figure 1.6a), and compared to the methylated POPOP laser dye (**1** in Figure 1.6a)⁶⁹. A short saturated hydrocarbon chain was used to separate the two systems to make the electron transfer process efficient. Here it is believed that the energy transfer between the laser-dye and covalently bound *trans*-stilbenzene works according to a Förster type energy transfer mechanism. After the energy transfer the laser-dye is back in the ground state, where the *trans*-stilbenzene will internally relax back to the ground-state after which the cycle can be

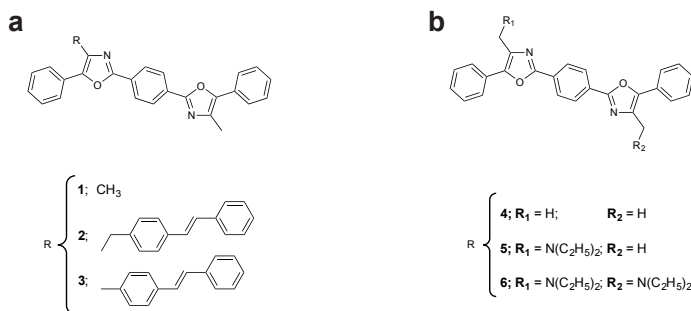


Figure 1.6 | Chemical structures of intramolecular photostabilized POPOP laser dyes. (a) POPOP laser dye linked to a *trans*-stilbenzene (**2** and **3**) to quench the triplet state⁶⁹. (b) POPOP laser dye linked to tertiary amines (**5** and **6**) to diminish the reactivity of singlet-oxygen⁷¹. (Figure adapted from Lüttke and co-workers^{69,71}).

repeated. An increase in the photophysics (brightness and photostability) of up to 500% for the photostabilizer-laser dye conjugates was observed.

To prevent photodamage caused by singlet oxygen the POPOP laser dye was equipped with singlet-oxygen scavengers (**5** and **6** in Figure 1.6)⁷¹. In Figure 1.6b the different POPOP laser dye derivatives with singlet oxygen scavengers are shown; here tertiary amines were used to quench singlet oxygen⁴⁴. Amines are known to be reactive towards singlet oxygen. Here the mechanism of deactivation of singlet oxygen is believed to occur via (radiationless) charge transfer deactivation mechanism where initially a singlet complex of the quencher and oxygen molecules is formed followed by transfer of electric charge to the oxygen molecule within the formed complex. Subsequently, inter-system crossing to a triplet ground state complex occurs which finally dissociates without charge-separation to triplet-oxygen and the tertiary amine^{44,72,73}. It is important to note that also a chemical reaction can occur between the tertiary amine and singlet-oxygen after which the the laser-dye is no longer protected from singlet-oxygen. It was observed that a ~50% decrease in photodamage could be obtained upon linking the laser-dye to tertiary amines.

Such photostabilizer-dye conjugates with intramolecular triplet-state quenching and or scavenging of singlet oxygen have "self-healing" or "self-protecting" properties (Figure 1.5b). More recently, Blanchard and co-workers⁷⁴⁻⁷⁷ and us (Chapter 2-6)⁷⁸⁻⁸¹ revived the strategy set out by Lüttke and colleagues⁶⁹⁻⁷¹ to improve the photostability of organic fluorophores that are widely used in single-molecule studies.

Blanchard and co-workers developed a method to improve the photophysics of cyanine dyes by linking them to known photostabilizers such as COT, Trolox (Figure 1.4e,f) and nitrophenyl alcohol⁷⁴⁻⁷⁷. Bi-functional Cyanine dyes were used as a linker between the (bio)molecular target and the triplet-state quencher (Figure 1.7a). It was shown that the photostabilizer-cyanine dye constructs reduced blinking and increased the photostability compared to the parent non-stabilized dye (Figure 1.7b). The improved photostability of the class of cyanine dyes by Blanchard and co-workers was, however, obtained under imaging conditions containing buffer additives (Fig-

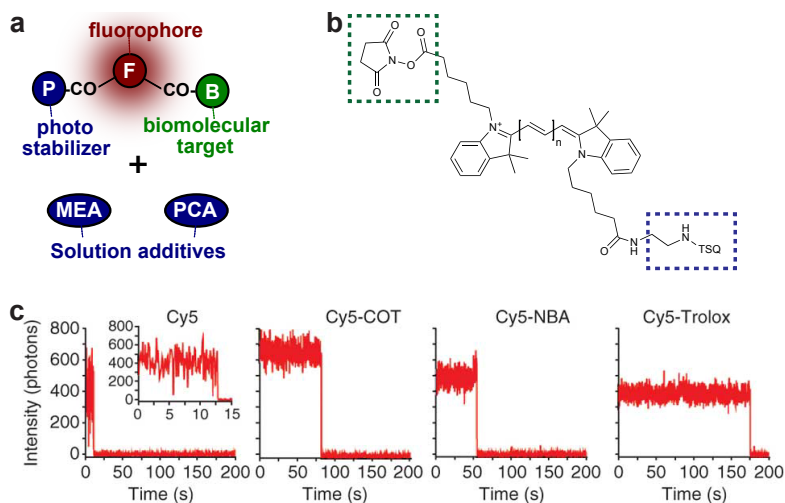


Figure 1.7 | Fluorophore scaffolding approach. (a) bis-reactive cyanine dye used to be linked to a photostabilizer (COT, NBA or Trolox) and a biomolecular target. Additionally, the solution additives used by Blanchard and co-workers are depicted. (b) Chemical structure (right) of a bis-reactive cyanine dye with in the dashed boxes indicated the functional groups to which the biomolecular target is linked (green, *N'*-hydroxide Succinimide ester, blue (Amide bond between the dye and TSO). (c) Fluorescent time traces of the different photostabilizer-Cy5 derivatives attached to dsDNA. (Figure adapted from Blanchard and co-workers⁷⁴).

ure 1.7a) known to influence and even improve the photostability (see Chapter 2⁷⁸; PCA and MEA (antioxidant) were present in the imaging buffer and as explained above MEA is used to quench the triplet state to suppress triplet-blinking. In these studies the effect of intramolecular photostabilization of the photostabilizer-dye conjugates were convoluted with diffusion-based quenching.

Thesis Outline

At this stage the use of intramolecular photostabilization in modern fluorescence microscopy was still of a "proof-of-principle" nature due to experimental problems and limitations of the chemical synthesis route that was needed to transform an organic fluorophore into a self-healing photostabilizer-conjugate. Hence, this represents the starting point of the work described in this thesis.

Limited scaffolding options. Blanchard and co-workers used the fluorophore itself as the linker between the (bio)molecular target and the photostabilizer which restricts the self-healing strategy to bis-reactive dyes such as shown in Figure 1.7b. These bis-reactive dyes are, however, rarely commercially available and only for a limited number of classes of organic fluorophores. As a result improved photostability with photostabilizer-dye conjugates was only available with limited number of fluorescent dyes.

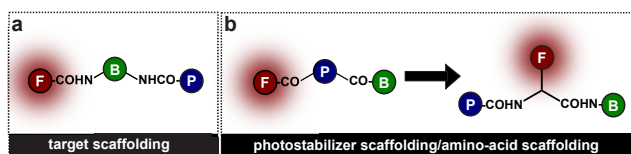


Figure 1.8 | Different scaffolding approached to connect an organic fluorophore, a photostabilizer and biomolecular target. (a) Fluorophore scaffolding. (b) Target scaffolding^{78,79,81}, (c) Photostabilizer scaffolding and amino-acid scaffolding⁸⁰.

Missing mechanistic models for photostabilization. While Lüttke and *co-workers* showed successful intramolecular photostabilization, however, it was still unclear whether a single photostabilizer can produce long-lasting and stable emission in single-molecule microscopy without the help of solution-additives. Furthermore, the quantitative performance of inter- vs. intramolecular photostabilization could not be evaluated from published studies due to use of buffer systems which contained the diffusion-based photostabilizer MEA. Mechanistically, experiments even suggested a distinct working mechanism of Trolox in inter- and intramolecular photostabilization⁷⁷. This work describes our progress in mechanistic understanding and new synthetic strategies of photostabilizer-dye conjugates. The synthetic strategies developed here differ from the fluorophore scaffolding approach that Blanchard and *co-workers*^{74,75,77} proposed by using either the target (target scaffolding, Figure 1.8a) or photostabilizer (photostabilizer scaffolding, Figure 1.8b) as the linker between the fluorophore, photostabilizer and (bio-)molecular target (Figure 1.8).

In the thesis we first report on the mechanism of intramolecular photostabilization in a direct comparison to photostabilization with solution additives (Chapter 2)⁷⁸. Studying the Cyanine fluorophore Cy5 linked to a photostabilizer on dsDNA as the biomolecular target shows that a proximal linked photostabilizer (Figure 1.8a) quenches the triplet state resulting in a non-blinking emission. Note, that no solution additives were added. The observed triplet state quenching is similar to that of diffusion-based triplet-state quenchers such as Trolox, COT and an ascorbic acid/methyl viologen (ROXS) mixture. The photostability, however, remains lower compared to diffusion-based methods and additionally the heterogeneity of sample increased. Adding a mixture of MEA/PCA results in single-molecule photoswitching instead of an increased photostability as was described by Blanchard and *co-workers*. This photoswitching of photostabilizer-dye conjugates suggests the potential applicability in stochastic optical reconstruction microscopy (STORM) microscopy.

Next, new photostabilizers were developed (Chapter 3⁷⁹) for intramolecular photostabilization to be competitive with diffusion-based photostabilization. An intramolecular reducing oxidizing system (iROXS) was designed, synthesized and tested for inter- and intramolecular photostabilization. It was shown that iROXS as a solution additive has a similar photostabilization increase compared to (solution) ROXS. Moreover, intramolecular photostabilization with iROXS is competitive with (solution) ROXS.

To be able to test and eventually improve the photophysics of different classes of (commer-

cially) available organic fluorophores a new method was developed making use of unnatural amino acids (UUAs). The UUAs served as the photostabilizer that covalently linked the fluorophore and (bio)molecular target (Chapter 4). Using the unnatural amino-acid scaffolding approach different classes of organic fluorophores can be connected to different photostabilizers for intramolecular photostabilization: "self-healing" fluorophores. Photostabilization was obtained for a variety of classes of organic fluorophores using only NHS- or click chemistry. The fluorophores were used to label biomolecules - DNA, proteins and antibodies - and used in single single-molecule microscopy (Chapter 4⁸⁰), single molecule Förster resonance energy transfer (smFRET) microscopy (Chapter 4⁸⁰) and super-resolution (STED) fluorescence microscopy (Chapter 5).

Combined single molecule experiments and molecular dynamic simulations were used to understand the dynamics and mechanism of intramolecular photostabilization (Chapter 6)⁸¹. The simulations suggest that the relative geometry between the fluorophore and the covalently linked or proximal positioned photostabilizer is important to obtain a substantial photostabilization effect. Additionally, it was found that the chemical nature of the photostabilizer is of lesser importance compared to geometry and collision dynamics.

Finally, this work presents a discussion about ongoing and future perspectives in the directions of intramolecular photostabilization. Speculations and preliminary results on how a tandem of identical photostabilizers performs in intramolecular photostabilization and how intramolecular photostabilization is most efficiently combined with diffusion-based photostabilizers. Furthermore, a description will be given of how to improve the photophysics (brightness and photostability) of fluorescent proteins.

References

1. Moerner, W. E. & Kador, L. Optical detection and spectroscopy of single molecules in a solid. *Physical Review Letters* **62**, 2535–2538 (1989).
2. Yildiz, A. Myosin V Walks Hand-Over-Hand: Single Fluorophore Imaging with 1.5-nm Localization. *Science* **300**, 2061–2065 (2003).
3. Yildiz, A. & Selvin, P. R. Fluorescence imaging with one nanometer accuracy: Application to molecular motors. *Accounts of Chemical Research* **38**, 574–582 (2005).
4. Schütz, G. J., Schindler, H. & Schmidt, T. Single-molecule microscopy on model membranes reveals anomalous diffusion. *Biophysical Journal* **73**, 1073–1080 (1997).
5. Xu, X. Direct Measurement of Single-Molecule Diffusion and Photodecomposition in Free Solution. *Science* **275**, 1106–1109 (1997).
6. Zhuang, X., Bartley, L. E., Babcock, H. P., Russell, R., Ha, T., Herschlag, D. & Chu, S. A Single-Molecule Study of (RNA) Catalysis and Folding. *Science* **288**, 2048–2051 (2000).

7. Kapanidis, A. N., Margeat, E., Ho, S. O., Kortkhonjia, E., Weiss, S. & Ebright, R. H. Initial transcription by RNA polymerase proceeds through a DNA-scrunching mechanism. *Science* **314**, 1144–1147 (2006).
8. McKinney, S. A., Déclais, A. C., Lilley, D. M. J. & Ha, T. Structural dynamics of individual Holliday junctions. *Nature Structural Biology* **10**, 93–97 (2003).
9. Stephens, D. J. & Allan, V. J. Light Microscopy Techniques for Live Cell Imaging. *Science* **300**, 82–86 (2003).
10. Gouridis, G., Schuurman-Wolters, G. K., Ploetz, E., Husada, F., Vietrov, R., de Boer, M., Cordes, T. & Poolman, B. Conformational dynamics in substrate-binding domains influences transport in the ABC importer GlnPQ. *Nature Structural & Molecular Biology* **22**, 57–64 (2014).
11. Moerner, W. E. A Dozen Years of Single-Molecule Spectroscopy in Physics, Chemistry, and Biophysics. *The Journal of Physical Chemistry B* **106**, 910–927 (2002).
12. Weiss, S. Fluorescence Spectroscopy of Single Biomolecules. *Science* **283**, 1676–1683 (1999).
13. Joo, C., Balci, H., Ishitsuka, Y., Buranachai, C. & Ha, T. Advances in single-molecule fluorescence methods for molecular biology. *Annual Review of Biochemistry* **77**, 51–76 (2008).
14. Lakowicz, J. R. *Principles of Fluorescence Spectroscopy Principles of Fluorescence Spectroscopy* (Springer, New York, 2006).
15. Sauer, M., Hofkens, J. & Enderlein, J. *Handbook of Fluorescence Spectroscopy and Imaging* (Wiley-VCH Verlag GmbH & Co. KGaA, Weinheim, Germany, 2011).
16. Hell, S. W. & Wichmann, J. Breaking the diffraction resolution limit by stimulated-emission - stimulated emission depletion fluorescence microscopy. *Optics Letters* **19**, 780–782 (1994).
17. Rust, M. J., Bates, M. & Zhuang, X. Sub-diffraction-limit imaging by stochastic optical reconstruction microscopy (STORM). *Nature Methods* **3**, 793–796 (2006).
18. Tsien, R. Y. The Green Fluorescent Protein. *Annual Review of Biochemistry* **67**, 509–544 (1998).
19. Giepmans, B., Adams, S., Ellisman, M. & Tsien, R. The Fluorescent Toolbox for Assessing Protein Location and Function. *Science* **312**, 217–224 (2006).
20. Resch-Genger, U., Grabolle, M., Cavaliere-Jaricot, S., Nitschke, R. & Nann, T. Quantum dots versus organic dyes as fluorescent labels. *Nature Methods* **5**, 763–775 (2008).

21. Michalet, X., Pinaud, F. F., Bentolila, L. A., Tsay, J. M., Doose, S., Li, J. J., Sundaresan, G., Wu, A. M., Gambhir, S. S. & Weiss, S. Quantum Dots for Live Cells, in Vivo Imaging, and Diagnostics. *Science* **307**, 538–544 (2005).
22. Ha, T. & Tinnefeld, P. Photophysics of Fluorescent Probes for Single-Molecule Biophysics and Super-Resolution Imaging. *Annual Review of Physical Chemistry* **63**, 595–617 (2012).
23. Levitus, M. & Ranjit, S. Cyanine dyes in biophysical research: the photophysics of polymethine fluorescent dyes in biomolecular environments. *Quarterly Reviews of Biophysics* **44**, 123–151 (2011).
24. Bosisio, C., Quercioli, V., Collini, M., D'Alfonso, L., Baldini, G., Bettati, S., Campanini, B., Raboni, S. & Chirico, G. Protonation and conformational dynamics of GFP mutants by two-photon excitation fluorescence correlation spectroscopy. *Journal of Physical Chemistry B* **112**, 8806–8814 (2008).
25. Adam, V., Carpentier, P., Violot, S., Lelimosin, M. L., Darnault, C., Nienhaus, G. U. & Bourgeois, D. Structural basis of X-ray-induced transient photobleaching in a photoactivatable green fluorescent protein. *Journal of the American Chemical Society* **131**, 18063–18065 (2009).
26. Bogdanov, A. M., Mishin, A. S., Yampolsky, I. V., Belousov, V. V., Chudakov, D. M., Subach, F. V., Verkhusha, V. V., Lukyanov, S. & Lukyanov, K. A. Green fluorescent proteins are light-induced electron donors. *Nature Chemical Biology* **5**, 459–461 (2010).
27. Schwille, P., Kummer, S., Heikal, A. A., Moerner, W. E. & Webb, W. W. Fluorescence correlation spectroscopy reveals fast optical excitation-driven intramolecular dynamics of yellow fluorescent proteins. *Proceedings of the National Academy of Sciences* **97**, 151–156 (2000).
28. Hendrix, J., Flors, C., Dedecker, P., Hofkens, J. & Engelborghs, Y. Dark states in monomeric red fluorescent proteins studied by fluorescence correlation and single molecule spectroscopy. *Biophysical Journal* **94**, 4103–4113 (2008).
29. Nienhaus, G. U. & Wiedenmann, J. Structure, dynamics and optical properties of fluorescent proteins: Perspectives for marker development. *ChemPhysChem* **10**, 1369–1379 (2009).
30. Schenk, A., Ivanchenko, S., Röcker, C., Wiedenmann, J. & Nienhaus, G. U. Photodynamics of red fluorescent proteins studied by fluorescence correlation spectroscopy. *Biophysical Journal* **86**, 384–394 (2004).
31. Hohng, S. & Ha, T. Near-Complete Suppression of Quantum Dot Blinking in Ambient Conditions. *Journal of the American Chemical Society* **126**, 1324–1325 (2004).

32. Wang, X., Ren, X., Kahen, K., Hahn, M. A., Rajeswaran, M., Maccagnano-Zacher, S., Silcox, J., Cragg, G. E., Efros, A. L. & Krauss, T. D. Non-blinking semiconductor nanocrystals. *Nature* **459**, 686–689 (2009).
33. Doose, S., Neuweiler, H. & Sauer, M. Fluorescence quenching by photoinduced electron transfer: A reporter for conformational dynamics of macromolecules. *ChemPhysChem* **10**, 1389–1398 (2009).
34. Chen, I. & Ting, A. Y. Site-specific labeling of proteins with small molecules in live cells. *Current Opinion in Biotechnology* **16**, 35–40 (2005).
35. Szent-Gyorgyi, C., Schmidt, B. A. F., Schmidt, B. A. F., Creeger, Y., Fisher, G. W., Zakel, K. L., Adler, S., Fitzpatrick, J. A. J., Woolford, C. A., Yan, Q., Vasilev, K. V., Berget, P. B., Bruchez, M. P., Jarvik, J. W. & Waggoner, A. Fluorogen-activating single-chain antibodies for imaging cell surface proteins. *Nature Biotechnology* **26**, 235–240 (2008).
36. Paige, J. S., Wu, K. Y. & Jaffrey, S. R. RNA mimics of green fluorescent protein. *Science* **333**, 642–646 (2011). NIHMS150003.
37. Dave, R., Terry, D. S., Munro, J. B. & Blanchard, S. C. Mitigating Unwanted Photophysical Processes for Improved Single-Molecule Fluorescence Imaging. *Biophysical Journal* **96**, 2371–2381 (2009).
38. Rasnik, I., McKinney, S. a. & Ha, T. Nonblinking and long-lasting single-molecule fluorescence imaging. *Nature Methods* **3**, 891–893 (2006).
39. Vogelsang, J., Kasper, R., Steinhauer, C., Person, B., Heilemann, M., Sauer, M. & Tinnefeld, P. A Reducing and Oxidizing System Minimizes Photobleaching and Blinking of Fluorescent Dyes. *Angewandte Chemie International Edition* **47**, 5465–5469 (2008).
40. Cordes, T., Vogelsang, J. & Tinnefeld, P. On the mechanism of trolox as antiblinking and antibleaching reagent. *Journal of the American Chemical Society* **131**, 5018–5019 (2009).
41. Buschmann, V., Weston, K. D. & Sauer, M. Spectroscopic study and evaluation of red-absorbing fluorescent dyes. *Bioconjugate Chemistry* **14**, 195–204 (2003).
42. Anslyn, E. V. *Modern Physical Organic Chemistry* (University Science Books, U.S., 2006).
43. Aitken, C. E., Marshall, R. A. & Puglisi, J. D. An Oxygen Scavenging System for Improvement of Dye Stability in Single-Molecule Fluorescence Experiments. *Biophysical Journal* **94**, 1826–1835 (2008).
44. Schweitzer, C. & Schmidt, R. Physical mechanisms of generation and deactivation of singlet oxygen. *Chemical Reviews* **103**, 1685–1757 (2003).
45. Toutchkine, A., Nguyen, D. V. & Hahn, K. M. Merocyanine dyes with improved photostability. *Organic Letters* **9**, 2775–2777 (2007).

46. Kassab, K. Photophysical and photosensitizing properties of selected cyanines. *Journal of Photochemistry and Photobiology B: Biology* **68**, 15–22 (2002).
47. Sies, H. & Menck, C. F. Singlet oxygen induced DNA damage. *Mutation Research* **275**, 367–375 (1992).
48. Davies, M. J. Reactive species formed on proteins exposed to singlet oxygen. *Photochemical & photobiological sciences : Official journal of the European Photochemistry Association and the European Society for Photobiology* **3**, 17–25 (2004).
49. N. J. Turro, V. R. & Scaiano, J. C. *Modern Molecular Photochemistry of Organic Molecules* (University Science Books, 2010).
50. Benesch, R. E. & Benesch, R. Enzymatic Removal of Oxygen for Polarography and Related Methods. *Science* **118**, 447–448 (1953).
51. Swoboda, M., Henig, J., Cheng, H. M., Brugger, D., Haltrich, D., Plumeré, N. & Schlierf, M. Enzymatic oxygen scavenging for photostability without pH drop in single-molecule experiments. *American Chemical Society Nano* **6**, 6364–6369 (2012).
52. Widengren, J., Chmyrov, A., Eggeling, C., Löfdahl, P. Å. & Seidel, C. A. M. Strategies to improve photostabilities in ultrasensitive fluorescence spectroscopy. *Journal of Physical Chemistry A* **111**, 429–440 (2007).
53. Pfiffi, D., Bier, B. A., Marian, C. M., Schaper, K. & Seidel, C. A. M. Diphenylhexatrienes as photoprotective agents for ultrasensitive fluorescence detection. *Journal of Physical Chemistry A* **114**, 4099–4108 (2010).
54. Cordes, T., Maiser, A., Steinhauer, C., Schermelleh, L. & Tinnefeld, P. Mechanisms and advancement of antifading agents for fluorescence microscopy and single-molecule spectroscopy. *Physical Chemistry Chemical Physics* **13**, 6699–6709 (2011).
55. Yanagida, T., Nakase, M., Nishiyama, K. & Oosawa, F. Direct observation of motion of single F-actin filaments in the presence of myosin. *Nature* **307**, 58–60 (1984).
56. Sheetz, M. P. & Koppel, D. E. Membrane damage caused by irradiation of fluorescent concanavalin A. *Proceedings of the National Academy of Sciences* **76**, 3314–3317 (1979).
57. Giloh, H. & Sedat, J. Fluorescence microscopy: reduced photobleaching of rhodamine and fluorescein protein conjugates by n-propyl gallate. *Science* **217**, 1252–1255 (1982).
58. Leslie, R. J., Saxton, W. M., Mitchison, T. J., Neighbors, B., Salmon, E. D. & McIntosh, J. R. Assembly properties of fluorescein-labeled tubulin in vitro before and after fluorescence bleaching. *Journal of Cell Biology* **99**, 2146–2156 (1984).
59. Von Trebra, R. & Koch, T. H. Dabco stabilization of coumarin dye lasers. *Chemical Physics Letters* **93**, 315–317 (1982).

60. Lemke, E. A., Gambin, Y., Vandelinder, V., Brustad, E. M., Liu, H. W., Schultz, P. G., Groisman, A. & Deniz, A. A. Microfluidic Device for Single-Molecule Experiments with Enhanced Photostability. *Journal of the American Chemical Society* **131**, 13610–13612 (2009).
61. Lambert, C. R. & Kochevar, I. E. Electron transfer quenching of the rose bengal triplet state. *Photochemistry and Photobiology* **66**, 15–25 (1997).
62. KAVARNOS, G. J. *Fundamentals a Photo-Induce Electron Transfer* (Wiley, New York, 1976).
63. Rehm, D. & Weller, A. Kinetics of Fluorescence Quenching by Electron and H-Atom Transfer. *Israel Journal of Chemistry* **8**, 259–271 (1970).
64. Huang, Z., Ji, D., Xia, A., Koberling, F., Patting, M. & Erdmann, R. Direct observation of delayed fluorescence from a remarkable back-isomerization in Cy5. *Journal of the American Chemical Society* **127**, 8064–8066 (2005).
65. Kasper, R., Heilemann, M., Tinnefeld, P. & Sauer, M. Toward ultra-stable fluorescent dyes for single-molecule spectroscopy. In *Proceedings of SPIE, Advanced Microscopy Techniques*, 6633–6671 (OSA, Munich, 2007).
66. Delicado, E. N., Ferrer, A. S. & Carmona, F. G. A kinetic study of the one-electron oxidation of Trolox C by the hydroperoxidase activity of lipoxygenase. *Biochimica et Biophysica Acta - General Subjects* **1335**, 127–134 (1997).
67. Vogelsang, J., Cordes, T. & Tinnefeld, P. Single-molecule photophysics of oxazines on DNA and its application in a FRET switch. *Photochemical & Photobiological Sciences* **8**, 486–496 (2009).
68. Vogelsang, J., Steinhauer, C., Forthmann, C., Stein, I. H., Person-Skegro, B., Cordes, T. & Tinnefeld, P. Make them Blink: Probes for Super-Resolution Microscopy. *ChemPhysChem* **11**, 2475–2490 (2010).
69. Liphardt, B., Liphardt, B. & Lüttke, W. Laser dyes with intramolecular triplet quenching. *Optics Communications* **38**, 207–210 (1981).
70. Liphardt, B. & Lüttke, W. Laserfarbstoffe, I Bifluorophore Laserfarbstoffe zur Steigerung des Wirkungsgrades von Farbstoff-Lasern. *Liebigs Annalen der Chemie* 1118–1138 (1981).
71. Liphardt, B., Liphardt, B. & Luttke, W. Laser-Dyes III: Concepts to Increase the Photostability of Laser-Dyes. *Optics Communications* **48**, 129–133 (1983).
72. Monroe, B. M. Quenching of singlet oxygen by aliphatic amines. *The Journal of Physical Chemistry* **81**, 1861–1864 (1977). arXiv:1011.1669v3.

73. Ouannes, C. & Wilson, T. Quenching of Singlet Oxygen by Tertiary Aliphatic Amines. Effect of DABCO. *Journal of the American Chemical Society* **90**, 6527–6528 (1968).
74. Altman, R. B., Terry, D. S., Zhou, Z., Zheng, Q., Geggier, P., Kolster, R. A., Zhao, Y., Javitch, J. A., Warren, J. D. & Blanchard, S. C. Cyanine fluorophore derivatives with enhanced photostability. *Nature Methods* **9**, 68–71 (2011).
75. Altman, R. B., Zheng, Q., Zhou, Z., Terry, D. S., Warren, J. D. & Blanchard, S. C. Enhanced photostability of cyanine fluorophores across the visible spectrum. *Nature Methods* **9**, 626–626 (2012).
76. Tinnefeld, P. & Cordes, T. 'Self-healing' dyes: intramolecular stabilization of organic fluorophores. *Nature Methods* **9**, 426–427 (2012).
77. Zheng, Q., Jockusch, S., Zhou, Z., Altman, R. B., Warren, J. D., Turro, N. J. & Blanchard, S. C. On the mechanisms of cyanine fluorophore photostabilization. *Journal of Physical Chemistry Letters* **3**, 2200–2203 (2012).
78. van der Velde, J. H. M., Ploetz, E., Hiermaier, M., Oelerich, J., De Vries, J. W., Roelfes, G. & Cordes, T. Mechanism of intramolecular photostabilization in self-healing cyanine fluorophores. *ChemPhysChem* **14**, 4084–4093 (2013).
79. van der Velde, J. H. M., Oelerich, J., Huang, J., Smit, J. H., Hiermaier, M., Ploetz, E., Herrmann, A., Roelfes, G. & Cordes, T. The Power of Two: Covalent Coupling of Photostabilizers for Fluorescence Applications. *The Journal of Physical Chemistry Letters* **5**, 3792–3798 (2014).
80. van der Velde, J. H. M., Oelerich, J., Huang, J., Aminian, A., Smit, J. H., Galiani, S., Kolmakov, K., Eggeling, C., Herrmann, A., Roelfes, G. & Cordes, T. A simple and versatile design concept for fluorophore-derivatives with intramolecular photostabilization. *Nature Communications* **7**, 1–15 (2016).
81. van der Velde, J. H. M., Uusitalo, J. J., Ugen, L.-J., Warszawik, E. M., Herrmann, A., Marrink, S. J. & Cordes, T. Intramolecular photostabilization via triplet-state quenching: design principles to make organic fluorophores "self-healing". *Faraday Discussions* **184**, 221–235 (2015).

